Gas-Phase Ionization Energetics, Electron-Transfer Kinetics, and Ion Solvation Thermochemistry of Decamethylmetallocenes, Chromocene, and Cobaltocene

Matthew F. Ryan,† David E. Richardson,*,† Dennis L. Lichtenberger,*,‡ and Nadine E. Gruhn‡

Department of Chemistry, The University of Florida, Gainesville, Florida 32611-2046, and Laboratory for Electronic Spectroscopy and Surface Analysis, Department of Chemistry, University of Arizona, Tucson, Arizona 85721

Received October 12, 1993®

The gas-phase free energies of ionization, $\Delta G_i°$, for Cp^*_2Mn, Cp^*_2Fe, Cp^*_2Ni, Cp^*_2Os, Cp_2Cr, and Cp_2Co (Cp = η^5-cyclopentadienyl, Cp* = η^5-pentamethylcyclopentadienyl) have been determined by using the electron-transfer equilibrium (ETE) technique and Fourier transform ion cyclotron resonance mass spectrometry. The high-resolution valence photoelectron spectra of bis(benzene)chromium(0), Bz_2Cr, Cp^*_2Os, and Cp^*_2Ru have also been measured. Most of the $\Delta G_i°$ values are referenced to the estimated $\Delta G_i°$ value of Bz_2Cr, for which the narrow first ionization band at 5.473 ± 0.005 eV is assigned as the adiabatic ionization potential. The $\Delta S_i°$ for ionization of Bz_2Cr is assumed to be equal to the electronic entropy change, $\Delta S_{elec}°$ (=1.4 cal mol^{-1} K^{-1}), and the difference between the integrated heat capacities for Bz_2Cr and Bz_2Cr^+ is also assumed to be negligible near room temperature ($\Delta H_{i,0}° \approx \Delta H_{i,350}°$), leading to $\Delta G_i°(Bz_2Cr)$ = 125.6 ± 1.0 kcal mol^{-1}. Through the use of thermochemical cycles, estimates are given for the average heterolytic and homolytic M–Cp bond disruption enthalpies of $Cp_2Cr^{+/0}$ and $Cp_2Co^{+/0}$. Cyclic voltammetry experiments (CH_3CN/0.1 M Bu_4NPF_6) for the decamethylmetallocenes, including Cp^*_2Ru, were performed in order to determine differential solvation energies, $\Delta\Delta G_{solv}°$, for the +/0 redox couples. Generally, $\Delta\Delta G_{solv}°$ values for the decamethyl derivatives are in the range −21 to −29 (±4) kcal mol^{-1}. Electron-transfer kinetics for several metallocene couples were measured from the approach to equilibrium in the ETE experiments, and couples that involved Cp^*_2M compounds were observed to have rate constants less than 10% of the Langevin collision frequency when the free energy change was in the range 0 to −6 kcal mol^{-1}.

Many studies concerning the reactivity of metallocene complexes involve variations of substituents on the Cp (η^5-cyclopentadienyl) ligand, and substitution of Cp with Cp* (η^5-pentamethylcyclopentadienyl) is a common strategy for altering the electronic and steric properties of metallocenes.[1-4] Electronic effects due to permethylation of Cp ligands of metallocenes can be assessed by comparing the oxidation energetics of the Cp and Cp* metal complexes, and electrochemical potentials[5] and vertical ionization energies[6] have been determined for a number of Cp* complexes. However, if electrochemical oxidation/reduction for an organometallic complex is irreversible, the electrochemistry may not provide an accurate value for the thermodynamic potential. In addition, the intrinsic effect of permethylation on oxidation energies is modified by the differential solvation energies of the redox couples. Vertical ionization energies determined by valence photoelectron spectroscopy (PES) can be an accurate measure of the adiabatic ionization potential (aIP) if the equilibrium geometries of the ion and the neutral are similar.[7,8] The aIP is equivalent to the enthalpy of ionization at 0 K, $\Delta H_{i,0}°$. However, large structural differences between the neutral species and the ion can lead to broad peaks and an adiabatic ionization potential significantly different from the measured vertical ionization potential, as is the case for many of the decamethylmetallocenes.[6,9,10]

Gas-phase electron-transfer equilibrium (ETE) techniques have been used extensively to determine thermal free energies of ionization, $\Delta G_i°$, for metal complexes[11,12] and organic compounds.[13] We have previously reported ETE results for a number of metallocenes and substituted metallocenes with $\Delta G_i°$ values in the 6–7-eV range.[11,12a] In the present study, we have used Fourier transform ion

† University of Florida.
‡ University of Arizona.
® Abstract published in *Advance ACS Abstracts*, February 15, 1994.

(1) (a) Collman, J. P.; Hegedus, L. S.; Norton, J. R.; Finke, R. G. *Principles and Applications of Organotransition Metal Chemistry*, 2nd ed.; University Science Books: Mill Valley, CA, 1987. (b) *Comprehensive Organometallic Chemistry*, Wilkinson, G.; Stone, F. G. A., Abel, E. W., Eds.; Pergamon Press: Oxford, 1982. (c) Janiak, C.; Schumann, H. *Adv. Organomet. Chem.* **1991**, *33*, 291.

(2) (a) Robbins, J. L.; Edelstein, N.; Spencer, B.; Smart, J. C. *J. Am. Chem. Soc.* **1982**, *104*, 1882. (b) Duggan, D. M.; Hendrickson, D. N. *Inorg. Chem.* **1975**, *14*, 955.

(3) (a) Threlkel, R. S.; Bercaw, J. E. *J. Organomet. Chem.* **1977**, *136*, 1. (b) Fendrick, C. M.; Mintz, E. A.; Schertz, L. D.; Marks, T. J.; Day, V. W. *Organometallics* **1984**, *3*, 819.

(4) (a) Keske, G.; Lauke, H.; Mauermann, H.; Swepton, P. N.; Schumann, H.; Marks, T. J. *J. Am. Chem. Soc.* **1985**, *107*, 8091. (b) Jordan, R. F. *Adv. Organomet. Chem.* **1991**, *32*, 325. (c) Evans, W. J. *Adv. Organomet. Chem.* **1983**, *24*, 131.

(5) Kotz, J. C. In *Topics in Organic Electrochemistry*; Fry, A. J., Britton, W. E., Eds.; Plenum Press: New York, 1986.

(6) Green, J. C. *Struct. Bonding (Berlin)* **1986**, *43*, 37.

(7) Lias, S. G., Bartmess, J. A., Liebman, J. F., Holmes, J. L., Levin, R. D., Mallard, W. G., Eds. *Gas-Phase Ion and Neutral Thermochemistry*; American Institute of Physics: New York, 1988.

(8) (a) Rabalais, J. W. *Principles of Ultraviolet Photoelectron Spectroscopy*; Wiley-Interscience: New York, 1977. (b) Lichtenberger, D. L.; Kellogg, G. E. *Acc. Chem. Res.* **1987**, *20*, 379.

(9) (a) Cauletti, C.; Green, J. C.; Kelly, R.; Powell, P.; van Tilborg, J.; Robbins, J.; Smart, J. *Electron. Spectrosc. Relat. Phenom.* **1980**, *19*, 327. (b) Darsey, G. P. *Diss. Abstr. Int.* **1988**, *49*, 3750.

(10) Evans, S.; Green, M. L. H.; Jewitt B.; King, G. H.; Orchard, A. F. *J. Chem Soc., Faraday Trans. 2* **1973**, *70*, 356.

(11) Ryan, M. F.; Eyler, J. R.; Richardson, D. E. *J. Am. Chem. Soc.* **1992**, *114*, 8611.

0276-7333/94/2313-1190$04.50/0

cyclotron resonance mass spectrometry,[14] FTICR/MS, to determine thermal free energies of ionization for several decamethylmetallocenes, cobaltocene, and chromocene, which all have $\Delta G_i°$ values in the 5–6-eV range. The $\Delta G_i°$ values reported are for the oxidation process shown by eq 1, where L = Cp or Cp*. Free energies of ionization were

$$L_2M(g) \rightleftharpoons L_2M^+(g) + e^- \quad (1)$$

determined from the measured equilibrium constant for ETE reactions, and the lower energies are anchored to the estimated value of $\Delta G_i°$ for bis(benzene)chromium(0), Bz_2Cr, based on a combination of high-resolution photoelectron spectroscopy and statistical mechanics. This new reference compound provides a convenient and accurate anchor for ionization energetics of compounds with $\Delta G_i°$ values that are too low to bring readily to equilibrium with previously established reference compounds.

Photoelectron spectra are also reported here for Cp^*_2Os and Cp^*_2Ru. To our knowledge, a complete valence PES spectrum has not been reported previously for Cp^*_2Ru, and the new spectrum for Cp^*_2Os has increased resolution and better signal-to-noise than the previously published spectrum.[15] With these additional PES results, it is possible to compare the $\Delta G_i°$ values for all Cp* complexes in the ETE study with PES vertical ionization energies and band shapes.

Heterolytic and homolytic bond disruption enthalpies for M–Cp cleavage of $Cp_2Cr^{+/0}$ and $Cp_2Co^{+/0}$ are also derived from the gas-phase data by the application of thermochemical cycles.[11,16] Additionally, differential solvation energies, $\Delta\Delta G_{solv}°$, are estimated from a combination of $\Delta G_i°$ values and $E_{1/2}$ data for cobaltocene, chromocene, and several Cp^*_2M complexes.[2a, 15,17,18] The Born model for predicting $\Delta\Delta G_{solv}°$ values for $M^{+/0}$ couples has been applied previously to the metallocenes and other metal complexes.[11,19] The $\Delta\Delta G_{solv}°$ values for $Cp_2M^{+/0}$ and $Cp^*_2M^{+/0}$ couples are compared here to values estimated by the spherical Born model.

The rates of gas-phase electron-transfer (ET) for reactions of metallocenes were reported by our laboratory previously,[20] and rate constants for the ET process have been determined for many of the reactions in this study. The forward electron-transfer reaction is written in eq 2 so that the ETE reaction proceeds in an exoergic direction. We sought to investigate the roles of inner-sphere reorganizational barriers, free energy changes, and nonadiabaticity in these solvent-free reactions.

$$Cp^*_2M + R^+ \rightarrow R + Cp^*_2M^+ \quad (2)$$

Results

Gas-Phase Equilibrium Studies. Methods used for studying gas-phase electron-transfer equilibrium reactions have been described elsewhere.[11–13,21] The general reaction studied is shown in eq 3, where L_2M denotes a metallocene and R is a reference compound with a known $\Delta G_i°$ value. The free energy of reaction, $\Delta G_{et}°$, can be determined from

$$L_2M + R^+ \rightleftharpoons R + L_2M^+ \quad (3)$$

the measured K_{eq} for the ETE reaction. Equilibrium investigations using FTICR/MS are limited to reactions with $10^{-3} < K_{eq} < 1000$ ($|\Delta G_{et}°| < 5$ kcal mol^{-1}) due to limits on practically attainable partial pressure ratios. Partial pressure ratios in excess of 100 lead to K_{eq} values with large experimental uncertainty due to errors in the measured partial pressure of the minor component. The value of the ionization free energy for the metallocene at the experimental temperature, $\Delta G_{i,T}°$, can be determined provided the $\Delta G_{i,T}°$ value of R is known (eq 4).

$$\Delta G_{et}° = \Delta G_i°(L_2M) - \Delta G_i°(R) \quad (4)$$

We have introduced a new anchor ($Bz_2Cr^{0/+}$) for ETE studies of compounds with ionization energies in the 5–6-eV range. Because of the low values of the ionization potentials for the metallocenes studied,[6] suitable organic reference compounds for ETE were unavailable (organic reference compounds used in previous ETE studies have low $\Delta G_i°$ values approaching 140 kcal mol^{-1}).[7,11,13] Accordingly, several ionization free energy values reported here are anchored to the $\Delta G_i°$ of Bz_2Cr, 125.6 ± 1.0 kcal mol^{-1}. The adiabatic ionization potential of Bz_2Cr was determined through high-resolution photoelectron spectroscopy, and assumptions necessary to obtain $\Delta G_{i,350}°$ from the aIP are discussed later.

Figure 1 is an equilibrium ladder showing all ETE reactions investigated in this work. All $\Delta G_i°$ values lie adjacent to the complex formula, and free energy changes, $\Delta G_{et,350}°$, for specific reaction couples studied with an ICR cell temperature of 350 K are adjacent to the arrows. Free energies of ionization are presented in Table 1 along with $\delta\Delta G_i°$ values, which are the differences between $\Delta G_i°(Cp^*_2M)$ and $\Delta G_i°(Cp_2M)$[11] values for each metal M. Error limits for $\Delta G_{et}°$ values are estimated at ±1 kcal mol^{-1}, due largely to possible errors in the measured pressures of the neutral reagent gases. Each reaction was repeated at least three times and examined from both endoergic and exoergic directions to demonstrate that the equilibrium

(12) (a) Ryan, M. F.; Siedle, A. S.; Burk, M. J.; Richardson, D. E. *Organometallics* **1992**, *11*, 4231. (b) Sharpe, P.; Richardson, D. E. Submitted. (c) Sharpe, P.; Kebarle, P. *J. Am. Chem. Soc.* **1993**, *115*, 782. (d) Sharpe, P.; Eyler, J. R.; Richardson, D. E. *Inorg. Chem.* **1990**, *29*, 2779. (e) Meot-Ner (Mautner), M. *J. Am. Chem. Soc.* **1989**, *111*, 2830. (f) Dillow, G. W.; Nicol, G.; Kebarle, P. *J. Am. Chem. Soc.* **1989**, *111*, 5465. (g) Dillow, G. W.; Kebarle, P. *J. Am. Chem. Soc.* **1992**, *114*, 5742.

(13) (a) Lias, S. G.; Ausloss, P. *J. Am. Chem. Soc.* **1978**, *100*, 6027. (b) Lias, S. G.; Jackson, J. A.; Argenian, H.; Liebman, J. F. *J. Org. Chem.* **1985**, *50*, 333. (c) Mautner, M.; Nelsen, S. F.; Willi, M. R.; Frigo, T. B.; *J. Am. Chem. Soc.* **1984**, *106*, 7384. (d) Nelsen, S. F.; Rumack, D. T.; Mautner, M. *J. Am. Chem. Soc.* **1988**, *110*, 7945.

(14) For reviews of the ion cyclotron resonance technique, see: (a) Marshall, A. G. *Acc. Chem. Res.* **1985**, *18*, 316. (b) Eyler, J. R.; Baykut, G. *Trends Anal. Chem.* **1986**, *6*, 44. (c) Gross, M. L.; Rempel, D. L. *Science* **1984**, *226*, 261. (d) Comisarow, M. B. *Anal. Chim. Acta* **1985**, *178*, 1. Applications to coordination compounds: (e) Sharpe, P.; Richardson, D. E. *Coord. Chem. Rev.* **1989**, *93*, 59.

(15) O'Hare, D.; Green, J. C.; Chadwick, T. P.; Miller, J. S. *Organometallics* **1988**, *7*, 1335.

(16) (a) Sharpe, P.; Richardson, D. E. *J. Am. Chem. Soc.* **1991**, *113*, 8339. (b) Richardson, D. E.; Christ, C. S.; Sharpe, P.; Ryan, M. F.; Eyler, J. R. In *Bond Energetics in Organometallic Compounds*; Marks, T. J., Ed.; ACS Symposium Series 428; American Chemical Society: Washington, DC, 1990. (c) Richardson, D. E. In *Energetics of Organometallic Species*; Martinho Simões, J. A., Ed.; NATO Advanced Study Institute Series C; Kluwer: Dordrecht, The Netherlands, 1992; Vol. 367. (d) Buckingham, D. A.; Sargenson, A. M. In *Chelating Agents and Metal Chelates*; Dwyer, F. P., Mellor, D. P., Eds.; Academic: New York, 1986.

(17) Hollaway, J. D. L.; Gieger, W. E. *J. Am. Chem. Soc.* **1979**, *101*, 2038.

(18) Kolle, U.; Grub, J. *J. Organomet. Chem.* **1985**, *289*, 133.

(19) (a) Richardson, D. E. *Inorg Chem.* **1990**, *29*, 3213. (b) Krishtalik, L.; Alpatova, N. M.; Ovsyannikova, E. V. *Electrochim. Acta* **1991**, *36*, 435.

(20) Richardson, D. E.; Christ, C. S.; Sharpe, P.; Eyler, J. R. *J. Am. Chem. Soc.* **1987**, *109*, 3894.

(21) Eyler, J. R.; Richardson, D. E. *J. Am. Chem. Soc.* **1985**, *107*, 6130.

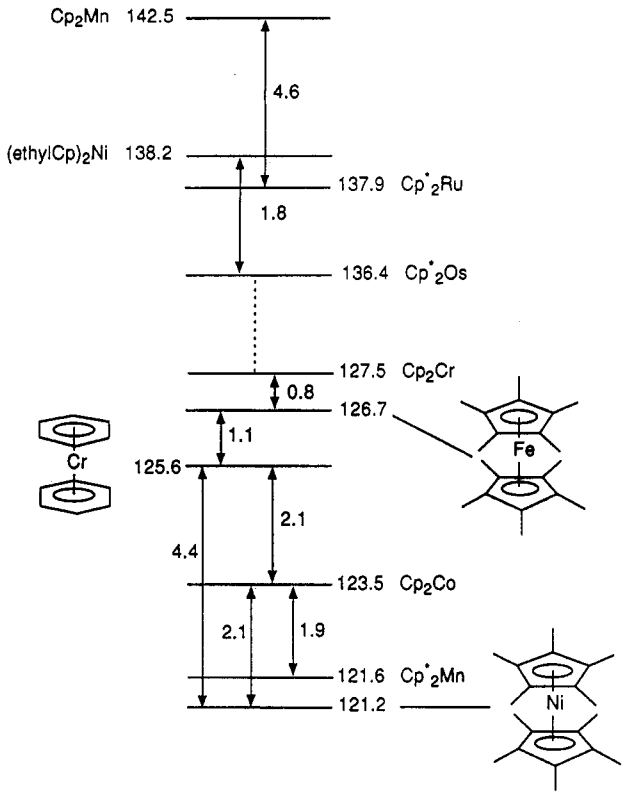

Figure 1. 1. Electron-transfer equilibrium ladder for several metallocenes. Values of $\Delta G_{et}°$ for individual ETE reactions are adjacent to arrows, and free energies of ionization, $\Delta G_i°$, are adjacent to the complex formulas. Free energy values are reported at 350 K and are anchored to the $\Delta G_{i,350}°$ value of bis(benzene)chromium.

Table 1. Ionization Energy Data for Some Metallocenes and Decamethylmetallocenes

L_2M	$\Delta G_i°$ [a]	vIP[b]	$\delta\Delta G_i°$ [c]
Cp^*_2Mn	121.6[d]	5.33 (122.9)[e]	
Cp_2Mn	142.5	6.26 (144.4)[e,f]	21
Cp^*_2Fe	126.7[d]	5.88 (135.6)[e]	
Cp_2Fe	153.1	6.88 (158.7)[g]	26
Cp^*_2Ni	121.2[d]	5.82 (134.2)[e]	
Cp_2Ni	143.8	6.51 (150.1)[g]	23
Cp^*_2Ru	137.9[d]	6.54 (150.8)[d]	
Cp_2Ru	164.6	7.45 (171.8)[h,i]	27
Cp^*_2Os	136.4[d]	6.31 (145.5)[d]	
Cp_2Os	160.6	7.15 (164.9)[j]	24
Cp^*_2Cr	(104)[k]	4.93 (113.7)[e]	
Cp_2Cr	127.5[d]	5.70 (131.4)[e]	(24)[k]
Cp^*_2Co	(100)[k]	4.705 (108.5)[e]	
Cp_2Co	123.5	5.55 (128.0)[e]	(24)[k]
Bz_2Cr	125.6[l]	5.473 (126.2)[d]	

[a] Units are kcal mol^{-1}. Estimated error limits ±1.5 kcal mol^{-1}, except as noted. Data for Cp_2M compounds from ref 11 except as noted. [b] Vertical ionization energies in eV (with kcal mol^{-1} in parentheses). [c] $\Delta G_i°(Cp_2M) - \Delta G_i°(Cp^*_2M)$ in kcal mol^{-1}. [d] This work. [e] Reference 9a. [f] Ion state is $^2E_{2g}$. vIP($^6A_{1g}$) = 6.91 eV. [g] Reference 6. [h] Average of spin–orbit components. [i] Reference 10. [j] Reference 30 ($^2E_{2(5/2)}$ ion state). [k] Estimated assuming that $\delta\Delta G_i°$ is average of first five entries. [l] See text. Estimated error limits ±1.0 kcal mol^{-1}.

constants obtained for the reactions were not dependent upon the direction of approach to equilibrium. Values of $\Delta G_i°$ for the metallocenes have estimated error limits of ±1.5 kcal mol^{-1}. One cross check was performed to test internal consistency, and the $\Delta G_{et}°$ values were consistent within ±0.2 kcal mol^{-1}. Most of the desirable cross checks could not be performed since both compounds would require introduction on the solids probe and reactant pressures could not be controlled separately.

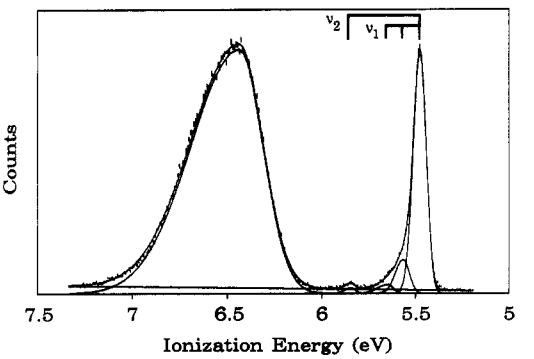

Figure 2. High-resolution He I photoelectron spectrum of bis(benzene)chromium(0) in the valence ionization region.

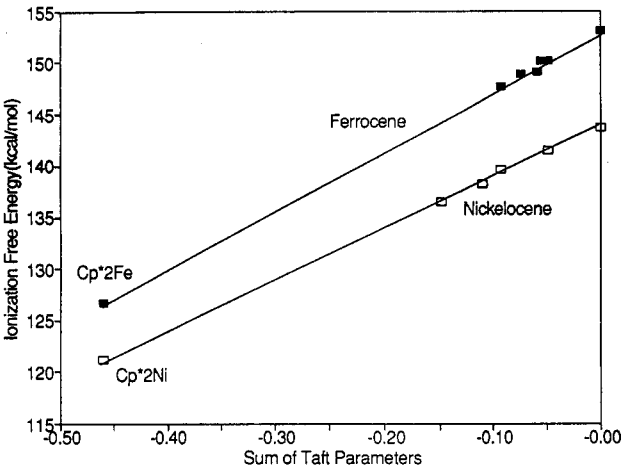

Figure 3. Plots of $\Delta G_i°$ for alkylferrocene and alkylnickelocene compounds versus sums of Taft σ_I parameters.

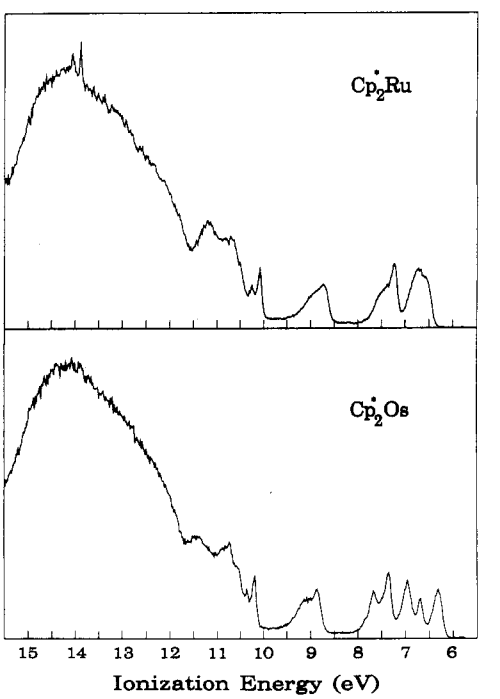

Figure 4. He I photoelectron spectra of decamethylruthenocene and decamethylosmocene.

Photoelectron Spectra. High-resolution valence photoelectron spectra of Bz_2Cr, Cp^*_2Os, and Cp^*_2Ru are shown in Figures 2 and 4–6. Lowest vertical ionization energies are summarized in Table 1.

Electrochemical Measurements. Table 2 lists the electrode potentials, $E_{1/2}$, of Cp^*_2Mn, Cp^*_2Fe, Cp^*_2Ni,

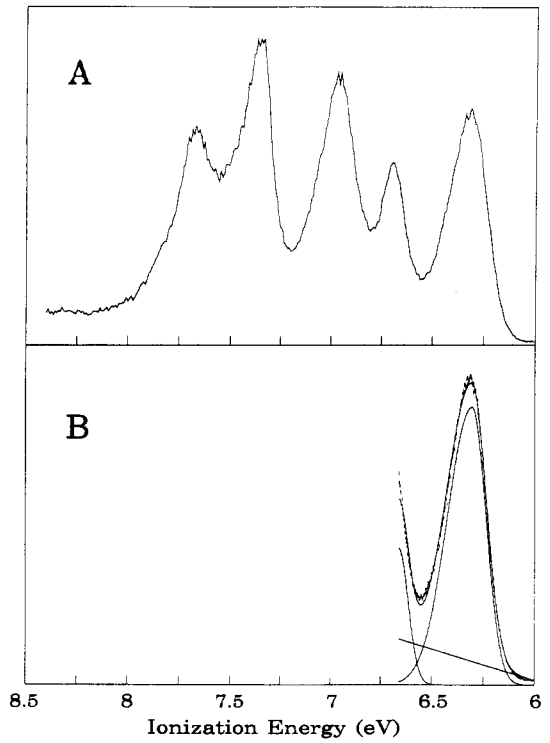

Figure 5. He I photoelectron spectra of decamethylosmocene. (A) Metal and ligand ionizations from 6 to 8.5 eV. (B) Close-up of the $^2E_{2(5/2)}$-state fit with asymmetric Gaussian peaks.

Table 2. Electrochemical $E_{1/2}$ Data and Differential Solvation Free Energies of Some $Cp^*_2M^{+/0}$ and $Cp_2M^{+/0}$ Couples

$Cp_2M^{+/0}$	lit. $E_{1/2}$[a] (solvent)	$E_{1/2}$[b] (this work)	$\Delta G_i°$(solv)[c]	$-\Delta\Delta G°_{solv}$[c]	δ_{Fc}[i]
Cp_2Cr	−0.67[d] (CH_3CN)		92	36	2
Cp_2Co	−0.94[d] (CH_3CN)		86	38	0
Cp^*_2Cr	−1.04[e] (CH_3CN)		84	(20)[f]	(18)
Cp^*_2Mn	−0.56[g] (CH_3CN)	−0.64	93	28	10
Cp^*_2Fe	−0.12[e] (CH_3CN)	−0.20	103	24	14
Cp^*_2Co	−1.47[e] (CH_3CN)		74	(26)[f]	(12)
Cp^*_2Ni	−0.65[e] (CH_3CN)	−0.69	92	29	9
Cp^*_2Ru	(CH_3CN)	0.41	117	21	17
Cp^*_2Ru	0.58[h] (CH_2Cl_2)	(0.09 vs Fc)	120	18	17[k]
Cp^*_2Os	0.46[l] (CH_2Cl_2)	(0.00 vs Fc)	118	18	17[k]

[a] Values reported in volts using 0.1 M Bu_4NBF_4 as supporting electrolyte against SCE, except chromocene and cobaltocene in 0.1 M Bu_4NPF_6 against SCE. [b] $E_{1/2}$ values determined in this work were measured in 0.1 M Bu_4NPF_6 in acetonitrile (or CH_2Cl_2 as noted) with ferrocene as an internal standard and then referenced against SCE ($E(Fc^{+/0})$ = 0.31 vs SCE for acetonitrile (solvent). When CH_2Cl_2 is solvent, values are reported against Fc reference. See text. [c] Units are kcal mol^{-1}. Estimated error limits ±4 kcal mol^{-1}. Calculated using $E_{1/2}$ values from this work when possible. [d] Reference 17. [e] Reference 2a. [f] Estimated from data in Table 1. [g] Reference 35. [h] Reference 22. [i] Derived using eq 9 in the text except where noted and assuming that $\Delta\Delta G_{solv}(Fc^{+/0})$ = −38 kcal mol^{-1} in acetonitrile. Values derived from eq 10 will differ slightly in some cases due to rounding errors. [j] Reference 15. [k] Using eq 10. For CH_2Cl_2, $\Delta\Delta G_{solv}(Fc^{+/0})$ = −35 kcal mol^{-1} is assumed (see ref 12a) to deduce $\Delta\Delta G_{solv}$ and ΔG_i from the value of δ_{Fc}.

and Cp^*_2Ru measured by cyclic voltammetry at a platinum disk electrode in acetonitrile containing 0.1 M *tert*-butylammonium hexafluorophosphate, Bu_4NPF_6, along with literature potentials when available. The $E_{1/2}$ of Cp^*_2Ru has been reported previously;[15,18,22] one value[22] measured in methylene chloride containing 0.1 M *tert*-butylammonium perchlorate is included in Table 2 along with our $E_{1/2}$ value vs $Fc^{+/0}$ measured in CH_2Cl_2 with 0.1 M Bu_4NPF_6. Values of $E_{1/2}$ in acetonitrile were also measured with ferrocene as an internal standard[23] and are tabulated against SCE assuming that $E°(Fc^{+/0})$ = 0.31 V vs SCE in acetonitrile to allow comparison to the literature values referenced against SCE.

(22) Gassman, P. G.; Winter, C. H. *J. Am. Chem. Soc.* **1988**, *110*, 6130.

Discussion

Bis(benzene)chromium(0). Most $\Delta G_i°$ values in this work are anchored to an estimated value for $\Delta G_i°(Bz_2Cr)$ as shown in Figure 1. Since this reference value is in the middle of the range for compounds studied, it provides a useful anchor in the 5–6-eV range. Bz_2Cr can be handled in air, is easily purified, and is sufficiently volatile to introduce via leak valves to obtain a working partial pressure. Previously used organic reference compounds have ionization energies in excess of 7 eV, and a large number of equilibria would be required in a ladder to reach the range of ionization energies covered here. With multiple equilibria, a decreasing confidence in the determined $\Delta G_i°$ values naturally arises as cumulative errors multiply. In this section, the PES experimental results and assumptions used to estimate $\Delta G_i°(Bz_2Cr)$ are discussed in detail to justify the choice of this organometallic as a new reference compound.

Figure 2 shows the high-resolution photoelectron spectrum of bis(benzene)chromium in the lower valence ionization region. Ionizations in the region from 6 to 7 eV can be assigned to the $^2E_2$ state of the cation (derived from ionization of the metal e_{2g} (d_{xy}, $d_{x^2-y^2}$) set). This band is very broad (fwhm 0.44 eV) due to unresolved vibrational fine structure along the ionization envelope. The sharp ionization at 5.473 ± 0.005 eV is due to the $^2A_1$ cationic state (correlating with removal of an electron from the predominantly metal a_{1g} (d_{z^2}) orbital).[6] The vertical ionization potential (vIP) is close to the literature value (5.45 eV).[6] The sharpness and lack of extensive vibrational structure are consistent with a nonbonding character for this ionization. The adiabatic ionization (fwhm 0.08 eV) is the most intense (vertical). Two short vibrational progressions of different frequencies are evident on this band and have not been reported previously. The weak shoulder near the base line on the high ionization energy side of the adiabatic ionization is best represented with two additional bands with spacing of 0.086 eV (697 ± 85 cm^{-1}, shown as ν_1 in Figure 2). This compares with the out of plane C–H bending mode (A_{1g}) found at 790 cm^{-1} in the Raman spectrum of $[Bz_2Cr]I$.[24a] In addition, there is a small feature at 5.843 eV, with a separation of 0.371 eV (3000 ± 60 cm^{-1}) from the vertical ionization. This corresponds to the symmetric C–H stretch (A_{1g}, shown as ν_2 in Figure 2) found at 3095 cm^{-1} in the Raman spectrum of $[Bz_2Cr]I$.[24a] The high signal-to-noise of the data allows these vibrational progressions to be seen. However, the low intensity of the vibrational bands compared to the vertical ionization again shows that there are only slight changes in geometry between the neutral and cationic species (consistent with the insignificant difference between Cr–C bond lengths in the crystal structures of Bz_2Cr and $[Bz_2Cr]I$[24b]). Similarly, there are only small changes in the vibrational frequencies between the neutral

(23) Gagne, R. R.; Koval, C. A.; Lisensky, G. C. *Inorg. Chem.* **1980**, *19*, 2855.

(24) (a) Fritz, H. P.; Lüttke, W.; Stammreich, H.; Forneris, H. *Spectrochim. Acta* **1961**, *17*, 1068. (b) Morosin, B. *Acta Crystallogr.* **1974**, *B30*, 838.

and cation species, as evidenced by comparison to the IR spectrum of Bz_2Cr.[25]

The value of $\Delta G_i°(Bz_2Cr)$ can be obtained from the adiabatic energy for the $^1A_1 \rightarrow {}^2A_1$ transition, estimates of the ionization entropy, and the integrated heat capacities of the neutral and ionic complexes. Ionization entropies for metal complexes have been estimated previously by using statistical mechanics.[11,26] For example, the value of $\Delta S_i°$ for $Cp_2Fe^{+/0}$ calculated from spectroscopic data is $\sim$5 cal mol^{-1} K^{-1} at 350 K, and the positive value is primarily due to changes in the vibrational and electronic entropies for the ferrocene couple (translational and rotational entropy changes were found to be only $\sim$0.1 cal mol^{-1} K^{-1} at 350 K, and $\Delta S_{vib}°$ accounted for nearly half of the total $\Delta S_i°$).[11] Sufficient spectroscopic data for bis(benzene)chromium and its cation do not exist to allow a complete statistical mechanical analysis; however, several important assumptions can be made in estimating a value for $\Delta S_i°(Bz_2Cr)$. First, the difference in the translational entropies for $Bz_2Cr^{+/0}$ will be negligible since changes in the molecular mass upon ionization are small. As inferred from the photoelectron spectrum, changes in the Cr–Bz metal–ligand bond length and ring bond lengths are minimal upon oxidation in the gas phase, and external rotation moments of inertia therefore do not change significantly (even compared to those of ferrocene, which has a much broader first ionization band and greater structural rearrangement upon ionization). The statistical mechanics study of the $Cp_2Fe^{+/0}$ couple revealed that vibrational frequency shifts isolated at the Cp rings (i.e., ring skeletal vibrations) were minor components of $\Delta S_{vib}°$, but shifts in metal–ligand vibrational frequencies (i.e., asymmetric and symmetric Fe–Cp stretch and Fe–Cp bend) significantly contributed to $\Delta S_{vib}°$.[11] Since metal–ligand vibrational frequencies change little between Bz_2Cr and Bz_2Cr^+,[25] $\Delta S_{vib}°(Bz_2Cr^{+/0}) \approx 0$ cal mol^{-1} K^{-1} will be assumed.

The largest estimated contribution to $\Delta S_i°$ for Bz_2Cr is the electronic ionization entropy, $\Delta S_{elec}°$. The ground-state configurations for Bz_2Cr and its cation are orbitally nondegenerate $^1A_1$ and $^2A_1$, respectively.[6] The electronic entropy change can then be determined from the change in electronic spin degeneracy given by $\Delta S_{elec}° = R(\ln 2)$. Therefore, the value for $\Delta S_i°(Bz_2Cr^{+/0})$ is estimated to be 1.4 cal mol^{-1} K^{-1} ($\Delta S_i° \approx \Delta S_{elec}°$) and, at 350 K, $T\Delta S_i° =$ 0.5 kcal mol^{-1}.

Changes in the integrated heat capacities for the $Bz_2Cr^{+/0}$ couple are also expected to be small. Statistical mechanical analysis has also been performed to estimate the change in the integrated heat capacities for the $Cp_2Fe^{+/0}$ couple, and values derived for $\Delta(H_T° - H_0°)$ are less than 1 kcal mol^{-1}, even up to 600 K.[11] By analogy, the differences in the integrated heat capacities for the $Bz_2Cr^{+/0}$ couple, from 0 to 350 K, are not expected to exceed 1 kcal mol^{-1}, and they probably are much lower since the critical M–Bz vibrational frequencies do not shift to the extent observed for the ferrocene couple. We then assume that aIP = 5.47 eV = $\Delta H_{i,0}° \approx \Delta H_{i,350}°$. Finally, $\Delta G_{i,350}° = 125.6 \pm 1.0$ kcal mol^{-1} can be derived from the estimated $\Delta H_{i,350}°$ and $\Delta S_{i,350}°$ values. The stated error of 1.0 kcal mol^{-1} encompasses estimated errors in the PES and statistical mechanical analysis.

(25) Saito, H.; Kakiuti, Y.; Tsutsui, M. *Spectrochim. Acta* **1967**, *23A*, 3013.

(26) (a) Richardson, D. E.; Sharpe, P. *Inorg. Chem.* **1991**, *30*, 1412. (b) Sharpe, P.; Richardson, D. E. *Inorg. Chem.* **1993**, *32*, 1809.

Cp^*_2M Free Energies of Ionization. As expected from previous PES studies,[6,9] methylation of the cyclopentadienyl rings lowers the ionization potential of the complexes with respect to the parent metallocenes. In a classical model, the polarizability and inductive[27] effects of the methyl groups stabilize the metallocene cation, leading to a lower ionization energy. In a quantum mechanical model, shifts in molecular orbital energies resulting from interactions between methyl groups and the Cp ring lead to a lower ionization energy with increased methyl substitution. Structural evidence for the increased electron-donating ability of pentamethylcyclopentadienyl ligand is clearly observed by a comparison of ruthenocene and Cp^*_2Ru. Crystal structures of Cp_2Ru and Cp^*_2Ru indicate that the M–Cp distance is 0.08 Å larger for ruthenocene than decamethylruthenocene.[22] The smaller M–Cp* distance for Cp^*_2Ru despite increased Cp*–Cp* repulsions can be rationalized by more electron rich Cp* rings being better donors to the Ru(II) metal center.

Generally, $\Delta G_i°$ values for the Cp^*_2M compounds studied here are 21–27 kcal mol^{-1} lower than those of their Cp analogues (note the $\delta\Delta G_i°$ entries in Table 1). The detailed effects of alkyl substitution on Cp_2M oxidation potentials will be different for each metal due to several factors, including the nature of the metal-based HOMO and different electronic degeneracies, but the relatively constant value of the shift in the $\Delta G_i°$ values on substitution of Cp* for Cp indicates that these differences are not large as the metal is varied.

The present ETE results for the Cp* complexes are consistent with previous results for alkylated metallocenes (e.g., $(C_5H_4R)CpFe$ and $(C_5H_4R)_2Ni$).[11,28] A plot of $\Delta G_i°$ values vs the sum of Taft σ_I parameters[29] is shown in Figure 3. The derived ρ values[11] from the slopes of the two plots shown in Figure 3 are 57 and 49 kcal mol^{-1} for ferrocene and nickelocene, respectively, demonstrating that ferrocene is somewhat more sensitive to alkylation than nickelocene. Predicted $\Delta G_i°$ values for Cp^*_2Fe and Cp^*_2Ni based on the previous Taft analyses for ferrocene and nickelocene alkylated derivatives[11,28] are within $\pm$1 kcal mol^{-1} of the experimentally determined values. Therefore, although $\delta\Delta G_i°(Cp^*_2M/Cp_2M)$ values for Fe and Ni are different, the Taft analyses indicates that our reported $\Delta G_i°$ values are consistent with $\Delta G_i°$ data for other alkyl substituents on nickelocene and ferrocene.

Discussion of the Photoelectron Spectra of Cp^*_2Ru and Cp^*_2Os. The full valence He I photoelectron spectra of Cp^*_2Ru and Cp^*_2Os are shown in Figure 4. The assignments of the ionizations follow from numerous previous investigations of the photoelectron spectra of metallocenes.[6] The electronic configurations of Cp^*_2Ru and Cp^*_2Os are the same as those of their unmethylated parent metallocenes. However, there are a few subtle differences which can be noticed in a detailed analysis of the metal valence d ionization region of these spectra. For several reasons it is easier to discuss the spectrum of Cp^*_2Os first.

(27) Discussions and references for alkyl group effects in are given in the following: (a) March, J. *Advanced Organic Chemistry*; Wiley-Interscience: New York, 1985; Chapters 8 and 9. (b) Lowry, T. H.; Richardson, K. S. *Mechanism and Theory in Organic Chemistry*, 3rd Ed.; Harper and Row: New York, 1987, Chapters 3 and 4.

(28) Richardson, D. E.; Ryan, M. F.; Khan, Md. N. I.; Maxwell, K. *J. Am. Chem. Soc.* **1992**, *114*, 10482.

(29) (a) Levitt, L. S.; Widing, H. F. *Prog. Phys. Org. Chem.* **1976**, *12*, 119. (b) Levitt, L. S.; Levitt, B. W. *Inorg. Nucl. Chem.* **1976**, *38*, 1907. (c) Parkanyi, C.; Levitt, L. S.; Levitt, B. W. *Chem. Ind. (London)* **1977**, 356.

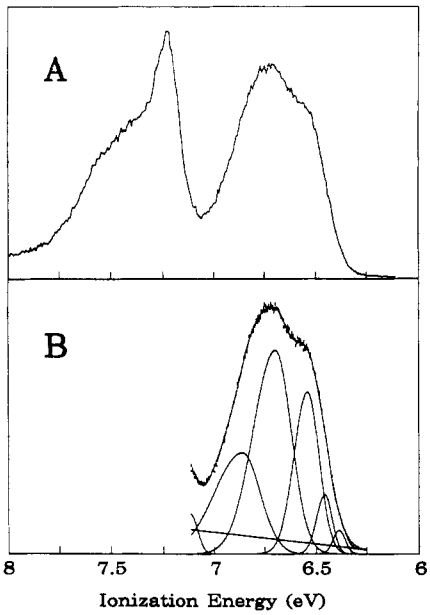

Figure 6. He I photoelectron spectra of decamethylruthenocene. (A) Metal and ligand ionizations from 6 to 8 eV. (B) Close-up of the metal band fit with asymmetric Gaussian peaks.

The He I and He II photoelectron spectra of Cp^*_2Os have been reported previously.[15] However, because of increased resolution and better signal-to-noise, a more detailed band profile analysis and accurate ionization positions are reported here. As shown in Figure 5, three distinct metal-based ionizations are observed in the low-valence region of Cp^*_2Os. The flanking ionizations are assigned as the spin–orbit split pair $^2E_{2(5/2)}$ state, at lowest ionization energy, and the $^2E_{2(3/2)}$ state, 0.66 eV to higher ionization energy (as measured from the vertical ionizations). The spin–orbit coupling parameter ξ is 0.33 eV for the $^2E_{2g}$ ionizations based upon these vertical ionization values. This is the same spin–orbit coupling observed in Cp_2Os.[30] The profiles of the ionization bands of Cp^*_2Os show evidence of unresolved vibrational fine structure, but not to the extent seen in Cp_2Os. The first ionization band of Cp^*_2Os is well represented with one Gaussian (Figure 5B).

Figure 6 shows a close-up spectrum of the metal ionization band of Cp^*_2Ru. In Cp_2Ru, this band comprises the $^2E_{2g}$ ionization, with a shoulder to the higher ionization energy side of the band which has been assigned previously as the $^2A_{1g}$ ionization. The metal band of Cp^*_2Ru has a very different shape from the metal band of Cp_2Ru. The first band of Cp^*_2Ru has a definite shoulder to the lower ionization energy side of the band. This shoulder must be the result of the intermediate spin–orbit coupling of ruthenium ($\lambda \approx 0.11$ eV[31]) which will split the metal e_{2g} set by about 0.2 eV. By analogy to osmocene and decamethylosmocene and in contrast to the previous assignment of ruthenocene, the first ionization is assigned to the $^2E_{2(5/2)}$ state of the spin–orbit split pair and the high binding energy side of the band is assigned to the $^2E_{2(3/2)}$ state of the pair. Due to the overlap of these ionizations with the $^2A_{1g}$ state, it is not possible to accurately assign the positions of the vertical ionizations.

(30) Lichtenberger, D. L.; Copenhaver, A. S. *J. Chem. Phys.* **1989**, *91*, 663.

(31) Griffith, J. S. *The Theory of Transition Metal Ions*; Cambridge: London, 1961.

The first ionization band is fitted in Figure 6B with the minimum number of Gaussians needed to fully represent the features of the band. Additional Gaussians are necessary to represent the band profile to the lower ionization energy side of the band due to the presence of vibrational structure.

Comparison of ETE Energies to Photoelectron Spectroscopy Results. In order to compare PES and ETE results it is necessary to estimate an adiabatic ionization enthalpy ($\Delta H_i°$) from the ETE data. With a negligible change in heat capacity for the ionization, the $\Delta H_i°$ value will then approximate the adiabatic ionization energy (aIP). Of course, it is unusual that aIP values can be deduced from valence PES results for organometallic complexes for comparison because of the broad unresolved bands usually encountered. The value of $\Delta H_i°$ for a compound can be deduced from temperature dependent ETE studies if an appropriate reference compound is available (with well-established $\Delta H_i°$ and $\Delta S_i°$ values). Otherwise, it can be estimated by a statistical mechanical correction to the free energy of ionization for the entropy of ionization ($\Delta H_i° = T\Delta S_i° + \Delta G_i°$). In the previous study[11] of the parent Cp metallocenes, the aIP from ETE estimated in this way (with $T\Delta S_i° \approx 2$ cal mol^{-1} K^{-1} at 350 K) agreed within experimental error with the aIP determined by a fit of the fine structure in the Cp_2Os PES spectrum.[30]

Comparison of $\Delta G_i°$ values for Cp^*_2M (M = Fe, Ru, Os) to the onset of the PES bands (Figures 4–6 and ref 9) for the first ionization shows that the free energies are well outside the Franck–Condon envelope of the PES band (ca. 0.2–0.3 eV lower in energy than the onset). Applying the approximate $T\Delta S_i°$ correction of ~2 kcal mol^{-1} (<0.1 eV) used for Cp_2Os[11] to these decamethyl complexes does not lead to $\Delta H_i°$ values within the PES band envelope. In contrast, for the parent Cp metallocenes[11] it is generally found that $\Delta H_i°$ values estimated from ETE studies lie within the lowest energy PES band envelope on the low-energy side of the vertical transition energy. Two explanations are possible for the different observation for the decamethyl complexes of Fe, Ru, and Os. First, the adiabatic transition may not be within the Franck–Condon envelope for the PES ionization due to a large displacement in excited-state bond lengths, or, second, the $T\Delta S_i°$ value may be larger in the decamethyl complexes, presumably due to larger contributions from shifts in vibrational frequencies involving the metal–Cp* bonds. Both explanations may be contributing to some extent, and the role of entropy changes can be assessed in principle by temperature dependent ETE studies.

The vertical ionization energies from PES for Cp^*_2Mn and Cp^*_2Ni have been determined by Green and coworkers.[6,9a] The assigned electronic configuration for Cp^*_2Ni ($^3E_{2g}$) is the same as that of the simple metallocene. However, Cp^*_2Mn is primarily a low-spin $^2E_{2g}$ complex[9] ($a_{1g}^2e_{2g}^3$) rather than a high-spin $^6A_{1g}$ complex as observed for manganocene.[6] The PES of Cp_2Mn is extremely broad due to a significant geometry difference between cation and the neutral.[9,10] In comparison, the PES of Cp^*_2Mn is substantially different from that of manganocene and the first ionization band is quite narrow.[6,9] The $\Delta G_i°$ values in this work are in agreement with the estimated aIP values determined from the onset of the PES manifolds for Cp^*_2Mn and Cp^*_2Ni.[9a]

Table 3. Average Bond Disruption Enthalpies for Chromocene and Cobaltocene[a]

	$\Delta H_{het}°$		$\Delta H_{hom}°$	
	M^{3+}–Cp^-	M^{2+}–Cp^-	M^+–$Cp^•$	M–$Cp^•$
Cp_2Cr	600 ± 5	306 ● 4	91 ± 3	76 ± 2
Cp_2Co	646 ± 5	321 ± 4	101 ± 3	73 ± 2

[a] Units are kcal mol^{-1}. Auxiliary data used to determine average bond disruption enthalpies given here were taken from refs 7 and 32.

Cobaltocene and Chromocene. Because of their low IP values, we have been unable to report the $\Delta G_i°$ values for cobaltocene and chromocene until now. Estimates for thermochemical properties of the ions in previous publications were based on vertical ionization energies from PES.[11] The $\Delta G_i°$ values shown in Table 1 are in overall agreement with PES ionization data, and they are on the low-energy side of the PES band shape.[9,10] The ground state configuration for chromocene is $^3E_{1g}$, and its low value of $\Delta G_i°$ with respect to ferrocene can attributed to the removal of an essentially nonbonding unpaired electron from a 16e$^-$ open-shelled compound. Since cobaltocene ($a_{1g}^2e_{2g}^4e_{1g}^1$) has one unpaired electron in an antibonding e_{1g} orbital, the low ionization potential is also easily rationalized.

Bond Disruption Enthalpies. Thermochemical cycles that incorporate $\Delta G_i°$ data have been used before to derive bond disruption enthalpies and differential solvation free energies for metallocenes.[11] The assumptions required to combine free energy of ionization data referenced at 350 K with $\Delta H_{vap,298}°$ for metal sublimations and $\Delta H_{i,0}°$ bare metal ionization energies[32] have been discussed earlier[11,16] and will not be described here. The values for $\Delta H°$ of the reactions in eqs 5 and 6 represent *twice* the average homolytic M–Cp, $\Delta H_{hom}°$ (eq 5), and heterolytic, $\Delta H_{het}°$ (eq 6), bond disruption processes for metallocenes and metallocenium ions. Average values for

$$Cp_2M(g) \rightarrow 2Cp^•(g) + M^0(g) \quad (5a)$$

$$Cp_2M^+(g) \rightarrow 2Cp^•(g) + M^+(g) \quad (5b)$$

$$Cp_2M(g) \rightarrow 2Cp^-(g) + M^{2+}(g) \quad (6a)$$

$$Cp_2M^+(g) \rightarrow 2Cp^-(g) + M^{3+}(g) \quad (6b)$$

$\Delta H_{het}°$ and $\Delta H_{hom}°$ were derived[11,12] from the heats of formation for the respective ions and neutrals, estimated from vertical ionization energies[32] and $\Delta H_f°$ data for Cp_2Cr and Cp_2Co,[7] and are given in Table 3. Error limits for heterolytic M–Cp bond disruptions enthalpies are larger than homolytic disruption enthalpies due to the inclusion of extra thermochemical data necessary for $\Delta H_{het}°$ calculations.[11]

Values for $\Delta H_{het}°$ and $\Delta H_{hom}°$ for chromocene and cobaltocene are consistent with those for other first transition row metallocenes. Although $\Delta G_i°$ values for chromocene and cobaltocene are much lower than those for other first transition row metallocenes, bond disruption enthalpies are in the same range. Bond disruption enthalpies are dependent upon $\Delta G_i°$ ($\approx \Delta H_i°$) data for the complexes and $\Delta H_i°$ data for the bare metal ions. For example, $\Delta G_i°(Cp_2Fe)$ is 30 kcal mol^{-1} greater than $\Delta G_i°(Cp_2Co)$, yet $\Delta H_{het}°$ for Cp_2Co^+ is 53 kcal mol^{-1} larger than $\Delta H_{het}°$ for ferrocenium cation primarily because $\Delta H_f°(Co(3+),g) > \Delta H_f°(Fe(3+),g)$ by 88 kcal mol^{-1}. In terms of the thermochemical cycles, $\Delta H_i°$ values for the bare metal Cr and Co ions compensate for lower $\Delta G_i°$ values for Cp_2Cr and Cp_2Co relative to other metallocenes.

Estimates of $\Delta H_{het}°$ and $\Delta H_{hom}°$ for the decamethylmetallocenes could not be made due to lack of thermochemical data for the heats of formation of the Cp^*_2M complexes and pentamethylcyclopentadienide (Cp^{*-}).

Differential Solvation Energies. Differential solvation energies, $\Delta\Delta G_{solv}°$, for metallocene redox couples were determined from comparison of $\Delta G_i°(g)$ values to $G_i°(soln)$ values estimated from electrochemical data obtained at 298 K. As with thermochemical cycles for determining bond disruption enthalpies, considerations for combining gas-phase ionization free energies and $\Delta G_i°$(soln) values have been discussed previously.[11,16,19] Briefly, values of $E_{1/2}$ for the metallocenes and decamethylmetallocenes are used to estimate $\Delta G_i°(soln)$ values by using eq 7. An estimate for the absolute potential for the

$$\Delta G_i°(soln) = nF(E_{1/2} + E°_{abs}(SHE) + E°(ref)) \quad (7)$$

standard hydrogen electrode[33] of 4.44 V is added to $E_{1/2}$ values along with the potential for the reference electrode leading to an estimate for $\Delta G_i°(soln)$. Corrections for liquid junction potentials have not been made for $E_{1/2}$ values. Differential solvation free energies are then determined from eq 8 and are negative since solvation stabilizes the cation relative to the neutral. Entropy and

$$\Delta\Delta G_{solv}° = \Delta G_i°(soln) - \Delta G_i°(g) \quad (8)$$

heat capacity changes from 298 K to 350 K are small for the metallocene redox couples[11,16b] and will only lead to minor errors. The stationary electron convention is assumed for both gas-phase and solution redox couples, although at 298 K both the stationary and the thermal electron convention yield essentially the same $\Delta G_i°$ values.[34]

Data used to calculate $\Delta G_i°(soln)$ and $\Delta\Delta G_{solv}°$ values are shown in Table 2. The literature $E_{1/2}$ values for the decamethyl complexes were obtained from several sources[18,22,35] and in different electrochemical conditions; therefore, we redetermined the $E_{1/2}$ values for a more consistent comparison of the Cp_2^*Mn, Cp^*_2Fe, Cp^*_2Ni, Cp^*_2Ru, and Cp^*_2Os couples under uniform conditions in acetonitrile (Table 2). Differential solvation free energies for the decamethyl complexes were then determined using our $E_{1/2}$ values when possible and are given in Table 2. Data for the $E_{1/2}$ of Cp^*_2Ru and Cp^*_2Os measured in CH_2Cl_2 are included in Table 2 for comparison. Estimates of $\Delta G_i°(g)$ for Cp^*_2Cr and Cp^*_2Co were obtained from average $\delta\Delta G_i°$ values for the other Cp^*_2M couples (Table 1), and $\Delta G_i°(soln)$ values were determined from $E_{1/2}$ measurement by Robbins et al.[2a] Estimates of $\Delta\Delta G_{solv}°$ could then be made for Cp^*_2Cr and Cp^*_2Co.

The $E_{1/2}$ values for the decamethyl derivatives are cathodically shifted by $\sim$0.5 V ($\sim$12 kcal mol^{-1}) relative to those of the corresponding Cp_2M couples.[18] A larger shift is observed in the gas phase, with the Cp^*_2M ionization free energies 21–27 kcal mol^{-1} lower than those of the corresponding Cp metallocenes. As a result, the

(32) (a) Moore, C. E. Analysis of Optical Spectra, *Natl. Stand. Ref. Data Ser. (U.S., Natl. Bur. Stand.)* **1970**, *NSRDS–NBS 34*. (b) Lide, D. R. *Handbook of Chemistry and Physics*; CRC Press: Boca Raton, 1990.

(33) Trasetti, S. *Pure Appl. Chem.* **1986**, *58*, 955.

(34) Sharpe, P.; Richardson, D. E. *Thermochim. Acta* **1992**, *202*, 173.

(35) Smart, J. C.; Robbins, J. L *J. Am. Chem. Soc.* **1978**, *100*, 3936.

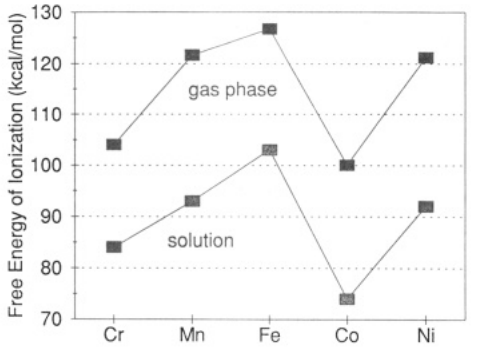

Figure 7. Plot demonstrating the periodic trend of ionization energies for the first transition row decamethylmetallocenes. Gas-phase data include $\Delta G_i°$ values determined in this work and estimated $\Delta G_i°$ values (Table 1). Solution $\Delta G_i°$ data (Table 2) were determined from $E_{1/2}$ values measured in acetonitrile in this work except for Cp^*_2Cr and Cp^*_2Co (ref 2a).

$-\Delta\Delta G_{solv}°$ values for $Cp^*_2M^{+/0}$ couples are ~9–17 kcal mol^{-1} smaller than those of the parent $Cp_2M^{+/0}$ couples.[11] As found for the Cp metallocenes,[11] the overall trends in $\Delta G_i°$ values as a function of metal M in the solution and the gas phase are similar (Figure 7).

It should be noted that the electrochemical measurements in this work were obtained with the ferrocene(+/0) couple as an internal reference. Furthermore, the gas-phase ionization free energy of ferrocene is known.[11] Thus, it is possible to quote differential solvation energies for the decamethyl couples relative to ferrocene *without requiring an absolute potential for the reference electrode.* We define this relative differential solvation energy, δ_{Fc}, in eq 9. A positive value of δ_{Fc} indicates that the redox

$$\delta_{Fc} = \Delta\Delta G_{solv}°(ML_n^{+/0}) - \Delta\Delta G_{solv}°(Fc^{+/0}) \quad (9)$$

couple has a less negative value of $\Delta\Delta G_{solv}°$ than $Fc^{+/0}$, i.e., the cationic member of the $ML_n^{+/0}$ couple is less stabilized relative to the neutral by solvation than is Fc^+ relative to Fc. Equation 10 can be derived from eqs 7–9.

$$\delta_{Fc} = F[E_{1/2}(ML_n^{+/0}) - E_{1/2}(Fc^{+/0})] + [\Delta G_i°(Fc,g) - \Delta G_i°(ML_n,g)] \quad (10)$$

Values of δ_{Fc} are given in Table 2 from data in Tables 1 and 2. The accuracy of these values depends only on the errors in determination of gas-phase and solution free energies of ionization relative to ferrocene, and the estimated errors are ±2 kcal mol^{-1}.

The Born equation, eq 11, has been used successfully for predicting ion solvation energies for $Cp_2M^{+/0}$ couples[11,16b] but apparently does not predict $\Delta G_{el}°$ values as accurately for Cp^*_2M complexes. The Born equation

$$\Delta G_{el}° = (-166z^2/r_{eff})(1 - 1/D) \text{ kcal mol}^{-1} \quad (11)$$

is used to estimate the change in electrostatic free energy, $\Delta G_{el}°$, when a charge z of sphere of radius r_{eff} is transferred from a vacuum to a sphere of equivalent radius in a medium of dielectric constant D (since there is little change in molecular dimensions on oxidation of metallocenes, $\Delta G_{el}° \approx \Delta\Delta G_{solv}°$). Differential solvation free energies predicted by combining eq 11 and the estimated average radii of the Cp^*_2M complexes are from 10% to 30% greater in magnitude than those derived from experiment. For example, the average molecular radius for decamethylferrocene is estimated to be ~5 Å,[36] and the estimated $\Delta G_{el}°$ (−32 kcal mol^{-1}) is more negative than the derived value of $\Delta\Delta G_{solv}°$ (−24 kcal mol^{-1}). Alternatively, the Born model predicts a molecular radius of 7.3 Å for Cp^*_2Fe based on the experimentally-derived solvation energetics. However, the eq 11 predictions for M = Mn and Ni are much closer to the experimental values, and the predicted values are within ~10% of the experimental values (as also found for the Cp metallocene couples[11]).

Table 4. Electron-Transfer Rate Constants for Some Metallocenes

	L_2M_a	L_2M_b	$-\Delta G_{et}°$ [a]	k_f [b]	k_f/k_L [c]
1	Cp^*_2Mn	Cp^*_2Ni	0	2.5×10^{-12}	0.002
2	Cp_2Cr	Cp^*_2Fe	1	6.7×10^{-11}	0.06
3	Cp^*_2Fe	Bz_2Cr	1	5.1×10^{-11}	0.05
4	Cp_2Co	Cp^*_2Mn	2	3.6×10^{-11}	0.03
5	Bz_2Cr	Cp^*_2Mn	4	6.7×10^{-11}	0.06
6	Bz_2Cr	Cp^*_2Ni	4	6.5×10^{-11}	0.06
7	Cp_2Cr	Cp^*_2Ni	6	7.4×10^{-11}	0.07
8	Cp^*_2Fe	Cp^*_2Ni	6	4.6×10^{-11}	0.04
9	Bz_2Cr	Cp_2Co	2	5.2×10^{-10}	0.52[d]
10	Cp^*_2Ni	Cp^*_2Ni	0	5.3×10^{-10}	0.48
11	Cp_2Ru	Cp^*_2Ni	43	3.8×10^{-10}	0.35

[a] All data for reaction direction $L_2M_a^+ + L_2M_b \rightarrow L_2M_a + L_2M_b^+$. Units are kcal mol^{-1}. [b] Units are cm^3 molecule^{-1} s^{-1}. [c] $k_L = 1.1 \times 10^{-9}$ cm^3 molecule^{-1} s^{-1} unless noted otherwise. See ref 20. [d] k_L estimated to be 1.0×10^{-9} cm^3 molecule^{-1} s^{-1} based on k_L for metallocene ET reactions.

The thermochemical radii for the decamethylmetallocene couples suggest that methylation can have an effect on solvation energetics beyond that modeled by a simple increase in the displacement of solvent by alkylation of the Cp ligand. It is apparent that the simple dielectric continuum/monopole model of eq 11 is inadequate for the case of M = Fe and Ru. A change in electron distributions in the metallocene upon methylation and the resulting change in the quadrupolar moments of the neutral molecule and its ion may lead to reduced solvation of the ion relative to the neutral in some cases, thereby increasing the Born thermochemical radius. Such an effect has also been suggested for poor modeling by eq 11 of solvation energetics in ruthenium tris(β-diketonate) complex +/0 redox couples.[12b]

The $\Delta\Delta G_{solv}°$ values for chromocene and cobaltocene are in agreement with other first transition row metallocenes.[11] A comparison of $\Delta\Delta G_{solv}°$ values indicates that a range of −36 to −39 kcal mol^{-1} is obtained for Cp_2M metallocenes with M = Cr, Fe, Co, and Ni.

Kinetics of Gas-Phase Electron-Transfer Reactions. Forward electron-transfer reaction rate constants from ETE studies were determined from the approach to equilibrium. Several electron-transfer reactions of decamethylmetallocene couples were observed in which ETE data could not be obtained because the approach to equilibrium was hampered by inefficient reaction kinetics and ion loss from the reaction cell.[20] Electron-transfer reaction rate constants for selected reaction couples are presented in Table 4. A detailed discussion for determining second-order rate constants for gas-phase electron-transfer reactions has been given elsewhere,[20] and similar methods have been used here.

The barrier for the electron-transfer process involving decamethylmetallocenes is expected to be similar to that

(36) Freyberg, D. P.; Robbins, J. L; Raymond, K. N.; Smart, J. C. *J. Am. Chem. Soc.* **1979**, *101*, 892.

for simple metallocenes.[37] Nevertheless, reaction rates in ETE experiments ($-\Delta G_{et} < 6$ kcal mol^{-1}) involving Cp^*_2M couples were typically an order of magnitude slower than for the Cp metallocenes,[20] and reaction efficiencies ($\Phi \equiv k_f/k_L$, the forward rate constant relative to the estimated Langevin collision rate constant[38]) were all <0.1.

Electron-transfer reactions involving Cp^*_2Ni were very slow, and in most cases equilibrium reactions had to be followed for >10 s. For the Cp^*_2Ni/Cp^*_2Mn reaction, electron-transfer equilibrium was never observed even out to reaction times of 15–20 s. From ion intensity versus time plots, it was observed that the two ions were decaying at different reaction rates, which is indicative of a slow electron-transfer process. The driving force for the reaction is ~0 kcal mol^{-1}, so this cross reaction was expected to be inefficient compared to others with strongly negative free energy changes. For example, the driving force for the electron transfer reaction of Cp^*_2Ni with Cp_2Ru^+ is −43 kcal mol^{-1} and the measured rate constant and efficiency (0.35) are in accord with other gas-phase electron-transfer reactions involving the ruthenocenium ion as the oxidant.[20] Other cross reactions with Cp^*_2Ni of lower driving force are not as efficient but are still readily followed to equilibrium (Table 4).

In view of the cross reaction data, the electron-transfer self-exchange reaction for the $Cp^*_2Ni^{+/0}$ couple was anticipated to be highly inefficient. Surprisingly, the self-exchange rate constant, $k_{se} = 5.3 \pm 1.0 \times 10^{-10}$ cm^3 molecule^{-1} s^{-1}, is not significantly different from the estimated maximum possible rate constant (the theoretical maximum rate constant for a metallocene self-exchange reaction is 5×10^{-10} cm^3 molecule^{-1} s^{-1} corresponding to $\Phi = 0.5$). The decamethylnickelocene self-exchange reaction clearly does not follow the trend between driving force and rate observed in its cross reactions (i.e., decreasing rate with decreasing driving force). It is possible that the "self-exchange" reaction is actually proceeding through an alternative pathway for exchange of the isotope label used to monitor the reaction (e.g., ligand exchange). Ligand exchange has been observed between neutral gas-phase labeled and unlabeled manganocenes[20] and may be expected for nickelocene and nickelocenium ions, which, like high-spin manganocene, have electrons in the antibonding e_g molecular orbital.

The inefficiency observed for the cross reactions of decamethylmetallocene couples despite small inner-sphere reorganizational barriers[20] may result from poor donor–acceptor orbital overlap in the ion-molecule precursor complex. A statistical rate theory study[39] suggested that poor electronic coupling between the initial and final states may be the cause of the subcollisional efficiency of the ferrocene–ferrocenium self-exchange reaction in the gas phase. The addition of methyl groups will further reduce electronic interactions between reactants (at least in most orientations), possibly accentuating the nonadiabaticity of this type of reaction (i.e., transmission coefficient $\kappa < 1$). On the other hand, the lower rates may reflect a change in the relative energetics of the reactants and the electron-transfer transition state. The effect of methylation on the potential surface controlling the electron transfer reaction is unknown, but the statistical models show that for a given inner reorganizational barrier the reaction rate is sensitive to the ion–molecule binding energy.[39] The latter is clearly modified by methylation of a metallocene, and a lower binding energy for this precursor complex could reduce the efficiency of the electron-transfer reaction.

(37) Richardson, D. E. *J. Phys. Chem.* **1986**, *90*, 3687.
(38) (a) Su, T.; Bowers, M. T. In *Gas Phase Ion Chemistry*; Bowers, M. T., Ed.; Academic Press: New York, 1979; Vol. 1, p 84. (b) Gioumousis, G.; Stevenson, D. P. *J. Chem. Phys.* **1958**, *29*, 294. (c) Su, T.; Chesnavich, W. J. *J. Chem. Phys.* **1982**, *76*, 5183. (d) Hu, S.; Su, T. *J. Chem. Phys.* **1986**, *85*, 1986.
(39) Richardson, D. E.; Eyler, J. R. *Chem. Phys.* **1993**, *176*, 457.

Conclusions

The ionization free energy for bis(benzene)chromium is a suitable anchor for electron-transfer equilibrium studies in the 5–6-eV range of ionization energies. It has a sharp first-ionization band in the PES that can be confidently assigned as the adiabatic ionization energy. Only the electronic entropy for conversion of the neutral species to the cation needs to be considered in the estimate of the adiabatic ionization free energy since structural and vibrational properties of the complex change little upon ionization.

Free energies of ionization for Cp^*_2Mn, Cp^*_2Fe, Cp^*_2Ni, Cp^*_2Ru, and Cp^*_2Os determined from gas-phase electron-transfer equilibrium techniques were found to be generally consistent with results of photoelectron spectroscopy. Additionally, $\Delta G_i°$ values for Cp^*_2Fe and Cp^*_2Ni were found to be consistent with $\Delta G_i°$ data for other alkylated metallocene complexes. The $\Delta G_i°$ values for the Cp^*_2M complexes with M = Fe, Ru, and Os are lower than the onset energies of the PES bands, indicating the advantage of the ETE method over PES in providing adiabatic energy data for use in thermochemical cycles. On the other hand, the PES data provide direct insight into the extent of structural distortion upon ionization as well as insights into electronic structure. It is clear that these two methods provide complementary data for describing the effect of ligand modifications on structure and reactivity of transition metal complexes.

Differential solvation free energies for chromocene and cobaltocene are in agreement with other first transition row metallocenes ($\Delta\Delta G_{solv}°$ in the range −36 to −39 kcal mol^{-1}). Thus, solvent interactions for the first transition row metallocenes continue to be predicted within ~10% by the simple spherical monopole Born model. As expected, the larger decamethyl compounds have less negative differential solvation free energies than the Cp metallocenes, with values for $\Delta\Delta G_{solv}°$ in the range −21 to −29 kcal mol^{-1} in acetonitrile. The spherical Born model predicts values of $\Delta\Delta G_{solv}°$ (ca. −32 kcal mol^{-1}) that are up to ~30% greater in magnitude than found experimentally.

Rate constants for electron-transfer reactions involving decamethyl complexes studied here are ~2–5% of the Langevin collision rate constant when the free energy change for the reaction is <6 kcal mol^{-1}. Although the apparent self-exchange reaction for Cp^*_2Ni is not inefficient, the electron-transfer reactions of Cp^*_2Ni with other metallocenes are very slow. The inefficiency in cross reactions may arise from poor electronic interaction between the reactants resulting from steric effects of the methyl groups. Alternatively, the reactions may be slowed by a reduction in the ion–molecule binding energy of the precursor complex.

Experimental Section

Electron-Transfer Equilibrium Investigations. Electron-transfer equilibrium studies were performed by using Fourier

transform ion cyclotron resonance mass spectrometry. The spectrometer utilized in the present studies is equipped with a 3T superconducting magnet and controlled by an Ionspec data station. Details of the mass spectrometer and electron-transfer experimental procedures have been described previously.[11,12,16]

Bis(benzene)chromium, cobaltocene, and chromocene were sublimed into the FTMS high-vacuum chamber through a heated Varian precision leak valve. Decamethylmetallocenes were introduced into the vacuum chamber by using a heated solids probe positioned adjacent to the reaction cell. When an equilibrium involving two Cp^*_2M complexes was investigated, the metallocene with the lower $\Delta G_i°$ (therefore requiring a lower neutral vapor pressure for equilibrium studies) was introduced through a heated leak valve and the second compound was sublimed from a heated solids probe. Typical reaction pressures were between 10^{-7} and 10^{-6} Torr for all ETE studies.

The temperature of the reaction cell was 350 K as measured by an Omega RTD thin film detector. Ions were produced through electron impact at 9–12 eV with a 20–30-ms beam event. Ions were thermalized through ion–molecule collisions (~30 collisions s^{-1}) prior to detection. Through the use of ion ejections, fragment ions could be removed from the cell before the ET reaction. Prior to the reaction period, one of the parent ions was ejected from the reaction cell and the population change of both parent ions with time was observed at set time intervals.

Partial pressures of the parent neutrals were measured directly with an ion gauge and then calibrated by using a Baratron capacitance manometer in the 10^{-5}-Torr range. Pressure corrections were extrapolated to experimental conditions in the 10^{-7}–10^{-6}-Torr range. Additional considerations concerning partial pressure measurements and pressure calibrations for our 3T FTMS system have been discussed in detail elsewhere.[40]

For kinetic studies, pressure corrections and normalizations for all molecular isotopes were performed prior to calculation of reaction rate constants. Corrections to account for diffusive loss of ions from the reaction cell were not performed as it was assumed that all ions were lost at essentially the same rate.[20] A home-made reaction cell with cell dimensions of 1.88 in. × 1.88 in. × 3.00 in., rather than the typical 1-in. cubic cell, was used for the majority of ETE and kinetic experiments. Ions could be trapped for ~5 s without significant loss of ion signal. Additionally, since more ions can be stored in a larger cell, reactions could be followed for longer reaction times, thus improving the accuracy of equilibrium constants obtained for reactions involving slow electron transfer.

Electrochemistry. Cyclic voltammetry studies were performed with a PAR system (Models 173/175). A platinum button working electrode and a Ag/AgCl reference electrode were used. Solvents used for electrochemistry were stored over molecular sieves for several days prior to purification. Acetonitrile (Fisher HPLC grade) was purified by shaking the solvent with CaH_2 and filtering, and then the solvent was distilled from P_2O_5 (5 g/100 mL) onto CaH_2 and redistilled from calcium hydride immediately prior to use. Pure methylene chloride (Fisher HPLC grade) was obtained by shaking with concentrated sulfuric acid, followed by an aqueous solution of Na_2CO_3, dried with anhydrous $CaCl_2$, filtered over neutral alumina, and stored over P_2O_5. Pure dry CH_2Cl_2 was obtained from distillation from P_2O_5 immediately prior to use. Bu_4NPF_6 (Aldrich) was recrystallized from ethanol/acetone three times, washed with dry ethanol, and dried in a vacuum oven at 100 °C for ca. 24 h. Electrolyte solutions were freshly prepared prior to all voltammetry studies.

Compounds. Decamethylnickelocene, decamethylmanganocene, decamethylosmocene, chromocene, cobaltocene, and bis(benzene)chromium were purchased from Strem Chemicals and used without further purification except for bis(benzene)-chromium, which was resublimed prior to use. Decamethylnickelocene is thermally unstable and after prolonged storage at ambient temperatures in an inert atmosphere required recrystallization. Decamethylferrocene and decamethylruthenocene were prepared according to literature procedures,[22,41] and their purity was evaluated by mass spectrometry and ^1H NMR.

Photoelectron Spectroscopy. The photoelectron spectra of Bz_2Cr, Cp^*_2Ru, and Cp^*_2Os were measured on an instrument built around a McPherson 36-cm-radius hemispherical analyzer (10-cm gap) with specially designed photon sources, ionization cells, power supplies, counter interface, and collection methods that have been described elsewhere.[42-44] The argon $^2P_{3/2}$ ionization at 15.759 eV was used as an internal calibration lock of the energy, and the CH_3I $^2E_{1/2}$ ionization at 9.538 eV provided an external calibration of the energy scale. During collection the instrument resolution (measured using fwhm of the Ar $^2P_{3/2}$ peak) was always better than 0.030 eV and was usually better than 0.025 eV. Spectra were obtained within a range of the following cell temperatures: Bz_2Cr, 82 ± 2 °C; Cp^*_2Ru, 72 ● 2 °C; and Cp^*_2Os, 76 ± 2 °C. Temperatures were measured via an Omega 217A digital thermometer equipped with a K-type thermocouple passed through a vacuum feedthrough and attached directly to the ionization cell. All samples vaporized cleanly, with no detectable evidence of decomposition products. All data were intensity-corrected with an experimentally determined instrument analyzer sensitivity function. Close-up spectra were also corrected for the He I β line spectrum, which is necessary because the source is not monochromatic.[45]

The data are represented analytically in terms of asymmetric Gaussian peaks. Each peak is defined by parameters representing the position of the peak, the half-widths on the high (W_h) and low (W_l) binding energy sides of the peak, and the amplitude of the peak as determined by the program FIT.[46] The first ionization band of Bz_2Cr is very sharp and intense, so that the reproducibility of this band position is at least ±0.005 eV. The ionization energies reported for the bands comprising overlapping ionizations generally are reproducible to about ±0.02 eV.

Acknowledgment. Work at the University of Florida was supported by a grant from the National Science Foundation (CHE9008663). D.L.L. acknowledges support of the Department of Energy (Division of Chemical Sciences, Office of Basic Energy Sciences, Office of Energy Research; Contract No. DE-FG02–86ER13501 for the study of the electronic structure of organometallic molecules), the National Science Foundation (CHE-8918959) for assistance in support of instrumentation, and the Materials Characterization Program (U. Arizona). The authors thank J. R. Eyler for helpful discussions.

OM9307040

(40) Bruce, J.; Eyler, J. R. *J. Am. Soc. Mass Spectrom.* **1992**, *3*, 727.

(41) (a) King, R. B.; Bisnette, M. B. *J. Organomet. Chem.* **1967**, *8*, 287. (b) King, R. B., Eisch, J. J., Eds. *Organometallic Syntheses*; Academic Press: New York, 1965.

(42) Calabro, D. C.; Hubbard, J. L.; Blevins, C. H., II; Campbell, A. C.; Lichtenberger, D. L. *J. Am. Chem. Soc.* **1981**, *103*, 6839.

(43) Lichtenberger, D. L.; Calabro, D. C.; Kellogg, G. E. *Organometallics* **1984**, *3*, 1623.

(44) Lichtenberger, D. L.; Kellogg, G. E.; Kristofzski, J. G.; Page, D.; Turner, S.; Klinger, G.; Lorenzen, J. *Rev. Sci. Instrum.* **1986**, *57*, 2366

(45) The He I β line is a secondary wavelength emitted by the He I source that causes a "shadow spectrum" shifted by 1.9 eV and at 3% the intensity of the He I α spectrum.

(46) Chandramouli, G. V. R.; Lalitha, S.; Manoharan, P. T. *Comput. Chem.* **1990**, *14*, 257.